Ultrasound in Med. & Biol. Vol. 15, No. 4, pp. 319–333, 1989
Printed in the U.S.A.

0301-5629/89 $3.00 + .00

●*Original Contribution*

CONTRAST AGENTS IN DIAGNOSTIC ULTRASOUND

JONATHAN OPHIR
Ultrasonics Laboratory, University of Texas Medical School, Department of Radiology, Houston, TX 77030
and
KEVIN J. PARKER
University of Rochester, Rochester Center for Biomedical Ultrasound, Rochester, NY 14627

(*Received* 30 *July* 1988; *in revised form* 7 *November* 1988)

Abstract—We review the field of contrast agents in diagnostic ultrasound. The progress in the development of various classes of contrast agents such as free and encapsulated gas bubbles, colloidal suspensions, emulsions, and aqueous solutions is described. The mechanisms for production of backscatter contrast, as well as attenuation contrast and speed of sound contrast are explained. Finally, the potential advantages and disadvantages of various classes of contrast agents are compared.

Key words: **Ultrasonic contrast agents, Backscatter enhancement, Contrast, Toxicity, Gas bubbles, Speed of sound, Attenuation.**

I. INTRODUCTION

Contrast enhancement is extensively used in clinical radiology. Modalities such as x-ray, CT, and nuclear medicine routinely rely on the introduction of foreign material into tissue in order to improve the contrast resolution in the image. The development of contrast materials in ultrasound, on the other hand, has been slow and sporadic, and to date there are no completely satisfactory materials for clinical imaging.

In this paper we review the progress which has been made in this field in the last two decades. We discuss various classes of materials which may be used as ultrasonic contrast agents. The physical mechanisms of contrast effects (backscatter, attenuation, and speed of sound) are described theoretically in order to quantify the potential merits and uses of these materials. In addition we cover some aspects of toxicity which are important to the development and ultimate use of contrast agents.

An ultrasonic contrast agent may be described as an exogenous substance which is introduced (usually) into the vascular system. The material could be in the form of solid particles in suspension, liquid droplets (emulsion), gas bubbles, encapsulated gases or liquids, or aqueous solutions. In order to be effective the materials must be stable throughout the examination, but metabolized or removed safely from the circulation shortly thereafter, and must also have preferential biodistribution and tissue uptake with relatively low toxicity, such that sufficient quantities can be administered. The acoustic properties of the material must give rise to altered acoustic echoes from tissue.

The principal acoustic parameters of tissue which may be influenced by the introduction of a contrast agent are the backscatter (echogenicity), attenuation, and/or the speed of sound propagation. Changes in backscatter may take the form of an increase or decrease in signal strength, and/or changes in the gray scale texture in the sonogram. Changes in attenuation may be inferred in cases where beam penetration is enhanced or diminished. Finally, the speed of sound in the organ may change. This change is typically small and cannot be appreciated in a normal sonogram; however, it may be quantitatively related to the amount of contrast material present in the tissue, and it might be detectable with special equipment.

Ultrasonic contrast agents could in principle be used for several purposes. Better contrast resolution between normal and diseased tissues may be attained via the use of contrast agents which have preferential uptake. Cavities and vessels may be outlined by contrast agents, especially during interventional procedures. Tissue characterization may also become feasible by selecting contrast agents which may be specific

for certain conditions. Doppler signals in blood flow measurements could be enhanced by contrast agents circulating in the vasculature. Finally, dynamic studies may be possible, which measure the rate of uptake and/or clearance of the agent in specific locations.

II. BACKGROUND

Reports which address the issue of ultrasound contrast agents have appeared in the literature since 1968, beginning with the use of free gas bubbles in echocardiology. Subsequent reports (1979–present) cover a multitude of other, more sophisticated types of contrast agents such as encapsulated gas bubbles, colloidal suspensions, liquid emulsions, and aqueous solutions.

1. *Free gas bubbles*

By far the simplest form of ultrasound contrast agents is free gas bubbles. Such bubbles may preexist in the liquid vehicle, or may be introduced via cavitation during the injection phase. Whatever the mechanism may be, it appears that almost any liquid, when rapidly injected into ducts or vessels, is capable of generating a quantity of air bubbles which may produce sufficient echoes to cause partial or complete intraluminal sonographic opacification.

The first report on the use of free gas bubbles appears to be that of Gramiak and Shah (1968) (Fig. 1). They obtained anatomic validation of the aortic origin of cardiac echoes by means of direct physiological saline injection during continuous echocardiographic recording. The injection produced a cloud of echoes which was delineated by the parallel signal of the aortic root. Kremkau et al. (1968) have again obtained intracardiac echoes from saline injection, but also from injection of autologous blood. This demonstrated that air bubbles may be generated during the injection process itself. Ziskin et al. (1972) have used a variety of liquids, such as renografin, carbonated water, and ether (which boils at body temperature) to demonstrate the presence of echoes in all cases, detected by enhanced Doppler signals from arteries. In recent years numerous investigators (Chiang et al. 1986; Rizayev and Azatyan 1985; Gillam et al. 1985; Meltzer et al. 1985; Feinstein et al. 1984; Kondo et al. 1984; Armstrong et al. 1984; Brown and Anderson 1984; Munoz et al. 1984; Tei et al. 1984; Levine et al. 1984; Ten-Cate et al. 1984; Maurer et al. 1984; Armstrong et al. 1983; Tei et al. 1983; Armstrong et al. 1982; Meltzer et al. 1981; Wise et al. 1981; Meltzer et al. 1980a; Meltzer et al. 1980b) have used gas microbubbles to study parts of the cardiovascular system. Additionally, other luminal structures have been opacified by gas bubbles. Specifically, Goldberg (1976) has used indocyanine green for opacification of the common bile duct in cholangiography. Presumably, microscopic air bubbles contained in the liquid or generated during the injection phase were responsible for the observed effects. Meyer-Schwickerath and Fritzsch (1986) have reported urologic applications of a new commercial agent which incorporates solid particles as microbubble carriers.

While free gas bubbles are extremely efficient scatterers of sound energy, their utility is limited by the fact that they are effectively removed by the lungs. Thus it would be impractical to use these to elicit

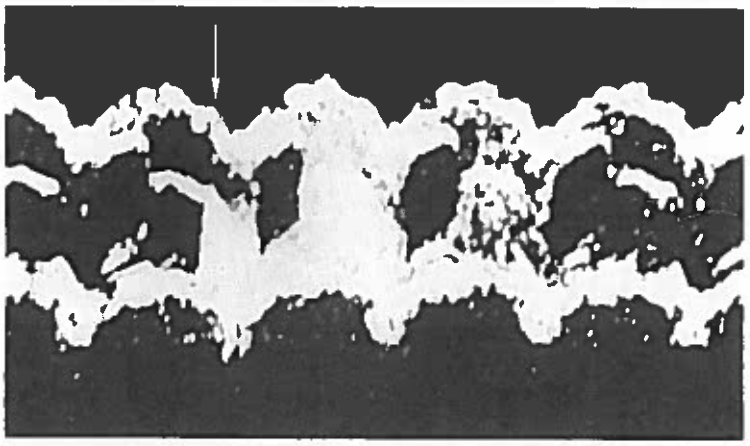

Fig. 1. Supravalvular aortic injection of saline in a patient with a normal aortic valve. Arrow denotes beginning of the injection. Note that resulting cloud is confined by margins of the aortic root. Rectangular defects in the echo pattern are caused by *non-contrast* blood entering the aorta from the ventricle during systole. Linear echoes between root margins arise from the aortic valve cusps. (Reprinted with permission from Gramiak and Shah 1968.)

contrast in the soft tissue via venous injection. However, intraarterial injection remains a possibility for localized contrast enhancement.

2. *Encapsulated gas bubbles*

In order to overcome some of the limitations of free gas bubbles, encapsulated gas bubbles were manufactured and injected directly into the carotid artery in tumor bearing rabbits (Carroll et al. 1980) (Fig. 2). These consisted of nitrogen gas trapped in 80 μm gelatin capsules. Carroll et al. report ultrasonic enhancement of tumor rims in rabbits with VX2 carcinoma. The large size of these particles did not allow their administration in the peripheral circulation. Unfortunately, the manufacture of small (2–3 μm), gas filled capsules which could clear the lungs is difficult due to the extreme thinness of the capsule wall through which gas diffuses. Thus the feasibility of this approach remains uncertain.

3. *Colloidal suspensions*

These preparations involve small solid particles suspended in a liquid vehicle. Several types of suspensions have been reported to date. Ophir et al. (1980) reported prolonged enhanced backscatter from canine livers *in vivo* using a peripheral injection of collagen microspheres with a 2 μm diameter (Fig. 3). This effect was hypothesized to occur due to agglomeration of scatterers in the Kupffer cells. Mattrey et al. (1982, 1983) reported a delayed and prolonged VX2 tumor rim enhancement in rabbit livers using a suspension of perfluorooctylbromide (PFOB) with particle sizes $\leq$ 0.5 μm. In addition, liver metastases not visible before were visualized in patients *in vivo* after administration of Fluosol-DA (Mattrey et al. 1987) (Figs. 4 and 5). Ophir et al. (1985) reported a 2 dB enhancement of canine liver backscatter obtained from 3 μm gelatin particles. Parker et al. (1987) reported enhancement of backscatter and attenuation in rat liver using a suspension of 1 μm particles of iodipamide ethyl ester (IDE) (Fig. 6). Colloidal suspensions appear to have the potential to produce contrast in the liver and the spleen. Since it has been shown that the particles are ultimately taken up by the Kupffer cells in the liver (Violante et al. 1980), pathologies such as some tumors which do not contain Kupffer cells would be expected to demonstrate lack of uptake of these agents. On the other hand, the size limitation for transpulmonary passage restricts backscatter efficiency, which is highly dependent on particle size, unless significant particle agglomeration occurs at the cellular site.

4. *Emulsions*

The idea of using liquid emulsions of certain lipids in aqueous vehicles was tested by Fink et al. (1985). Since it is known that fat deposition in hepatocytes produces enhanced backscatter from the liver, it might appear that such emulsions would cause a similar effect. Unfortunately, no enhancement of

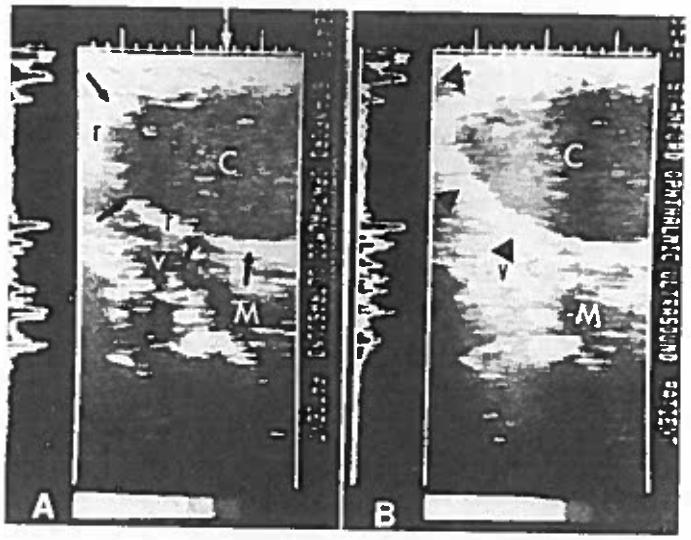

Fig. 2. (A) A control transverse scan of rabbit thigh and VX2 carcinoma demonstrating skin of rabbit (white arrow). VX2 carcinoma (black arrows) with relatively low echo center (C) and more echogenic rim (r) and a VX2 feeder vessel (v) approaching the tumor in normal muscle (M). (B) A second scan obtained without moving the transducer but following injection of 5 mL of 80 μm microbubbles. Increased echogenicity is seen in the tumor rim (arrow heads) and feeder vessels (v). No echo increase is observed in tumor center (C) or muscle (M). (Reprinted with permission from Carroll et al. 1980.)

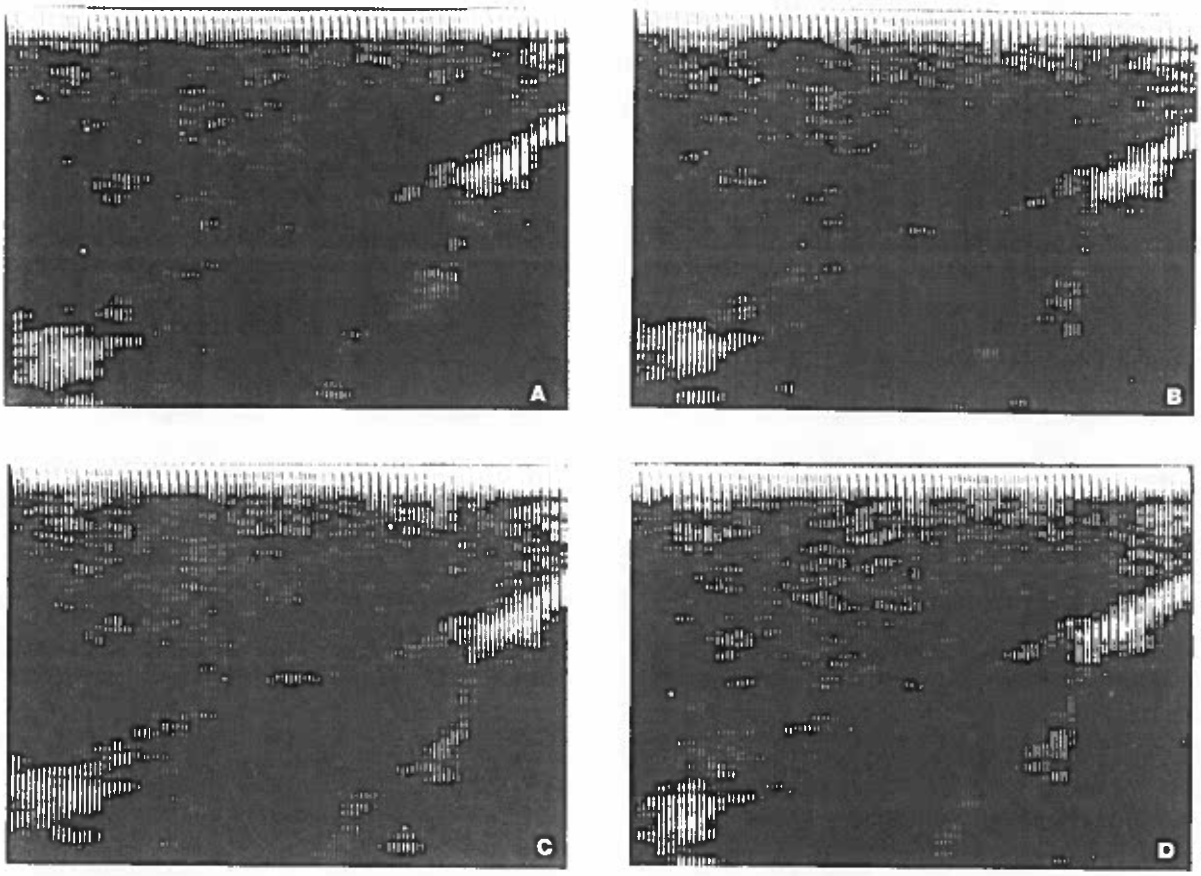

Fig. 3. Effects of collagen microsphere infusion on canine liver sonograms at 7 MHz. (A) Control; (B) 4 minutes following end of infusion; (C) 9 minutes following end of infusion: note observable backscatter enhancement throughout the liver; (D) 25 minutes following end of infusion: continued effect. (Reprinted with permission from Ophir et al. 1980.)

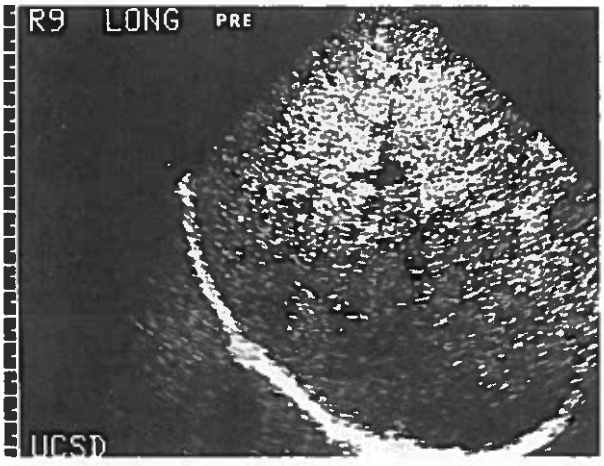

Fig. 4A. Patient with metastatic pancreatic carcinoma had an inhomogenous liver precontrast. A typical scan is shown. (Reprinted with permission from Mattrey et al. 1987.)

Fig. 4B. Liver enhancement following 2.4 g/kg Fluosol-DA 20% allowed the visualization of multiple clustered non-enhancing lesions (arrows). (Reprinted with permission from Mattrey et al. 1987.)

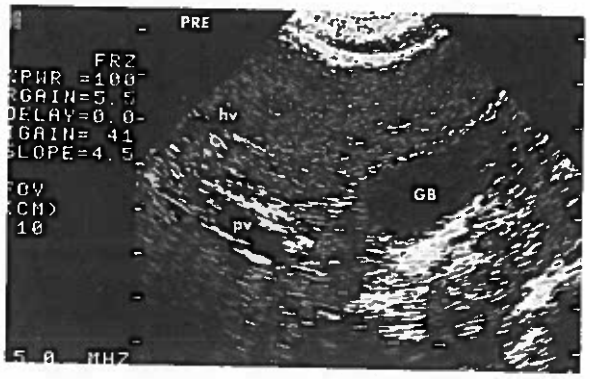

(A)

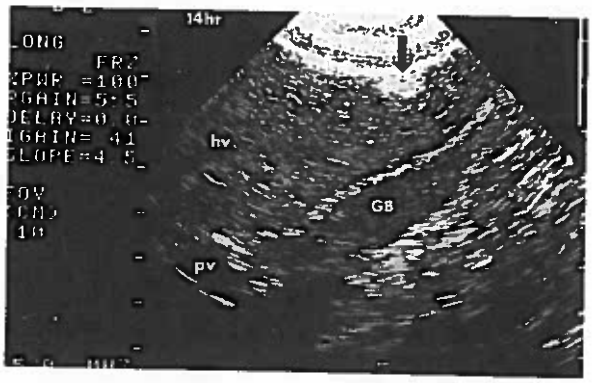

(B)

Fig. 5. Longitudinal scans obtained over the gallbladder (GB), portal vein bifurcation (pv), and hepatic vein (hv). (A) prior to contrasts, and (B) 14 hours following 2.4 g/kg Fluosol-DA 20%, at the same power and gain settings, in a patient with metastatic gastric carcinoma. Results show a 5 × 10 mm lesion (arrow) along the anterior surface of the liver not seen pre-Fluosol. (Reprinted with permission from Mattrey et al. 1987.)

backscatter was observable in these experiments. Fink et al. point out that the amount of lipid required to mimic fatty infiltration of the liver may be prohibitively high. Standard radiographic contrast agents were investigated by Banjavic et al. (personal communication, 1987) for this purpose, but no backscatter enhancement was noted.

5. *Aqueous solutions*

Backscatter enhancement due to administration of certain aqueous solutions into kidney tissue *in vitro* and *in vivo* was demonstrated by Ophir et al. (1979) (Figs. 7 and 8). The aqueous solutions of many compounds exhibit a linear increase in the speed of sound and density as a function of the molar concentration of the solute (McWhirt 1979). Hence the acoustic impedance is also a function of concentration. Based on these studies it was postulated that when a solution is initially introduced into the vascular system, transient acoustic impedance mismatches are created between the vascular and nonvascular beds (Ophir et al. 1979). This in turn gives rise to enhanced tissue backscatter. Suitable materials include buffered sodium citrate and calcium disodium EDTA in solution, which exhibit a strong dependence of the speed of sound on molarity (on the order of 200 m s^{-1} mol^{-1}) and a relatively low level of toxicity (Tyler et al. 1981).

III. BACKSCATTER CONTRAST MECHANISMS

By far the most important effect of contrast agents is the enhancement of backscatter (echogenicity) from tissue, since conventional ultrasound imaging relies on backscattered echoes for image generation. The strength of the backscatter is dependent on several factors, some of which depend on the experimental conditions, and others on the physical properties of the scatterer in relation to those of its surround.

1. *Long wavelength scattering*

Figure 9 shows the geometry which defines the scattering cross section of a scatterer. The total power P emitted by the circular transducer is assumed to be equally distributed over an area A in the plane which contains the scatterer, such that the intensity at this range is

$$I_i = P/A. \tag{1}$$

If the scatterer is much smaller than the ultrasonic wavelength (hence the term "long wavelength") it will produce a scattered wave which can be treated simply. If the scatterer presents only a speed of sound mismatch compared to the surrounding fluid, then a simple spherical wave is produced. If density mismatches are present, then a directivity pattern can result. In either case, total power scattered by the scatterer is defined by:

$$P_s = I_i \sigma \tag{2}$$

where σ is an area called the scattering cross section of the scatterer which is a measure of the scattering strength. In cases of spherical spreading of the scattered wave, the scattered intensity at a distance R from the scatterer is given as

$$I_s = I_i \sigma / 4\pi R^2, \tag{3}$$

and the power received by the receiving transducer of radius r at distance $R \gg r$ from the scatterer is therefore

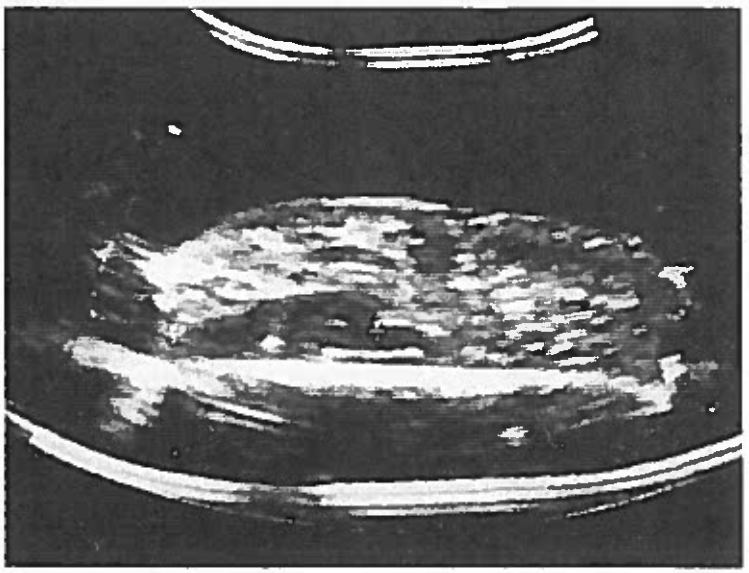

(A)

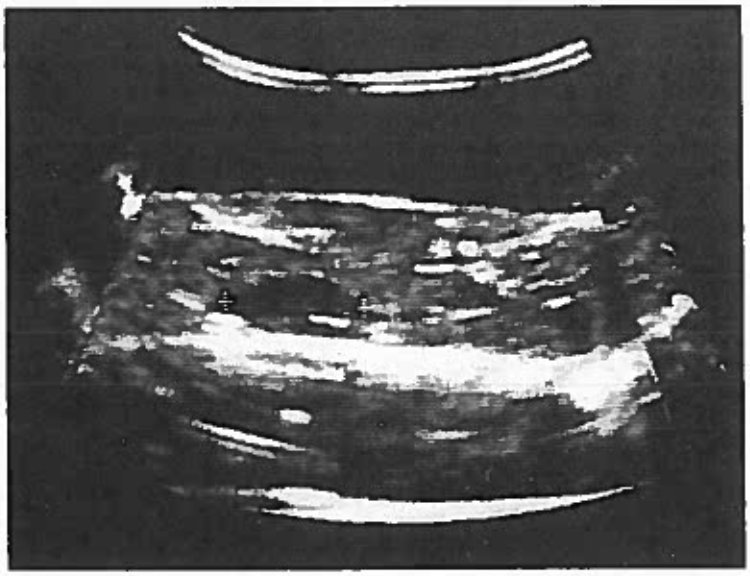

(B)

Fig. 6. B-scan images from a 7 MHz sector scanner, of IDE containing livers surrounding a single normal liver. The lobes are packed between plastic films, with the normal liver in the lower left quadrant, indicated by cursors. The normal liver appears hypoechoic compared to the livers with 3.2 mg/cc of 1.0 μm IDE particles. Parts (A) and (B) are different cross-sections of the packed liver layers. These images represent contrast enhancement of an initially isoechoic tumor region in liver. After particle uptake by surrounding normal parenchyma, the "tumor" is clearly defined as the hypoechoic region. (Reprinted with permission from Parker et al. 1987.)

$$P_r = I_s \pi r^2 = I_i \sigma r^2 / 4R^2. \quad (4)$$

Equation 4 demonstrates that the backscattered power received by the transducer is proportional to the scattering cross section of the scatterer.

The scattering cross section of a small scatterer is given by (Morse and Ingard 1968)

$$\sigma = \left[\frac{4}{9}\pi a^2 (ka)^4\right]\left[\left|\frac{\kappa_s - \kappa}{\kappa}\right|^2 + \frac{1}{3}\left|\frac{3(\rho_s - \rho)}{2\rho_s - \rho}\right|^2\right], \quad (5)$$

where

$k = 2\pi/\lambda$ = wave number, where λ is the wavelength,
a = radius of scatterer $\ll \lambda$,

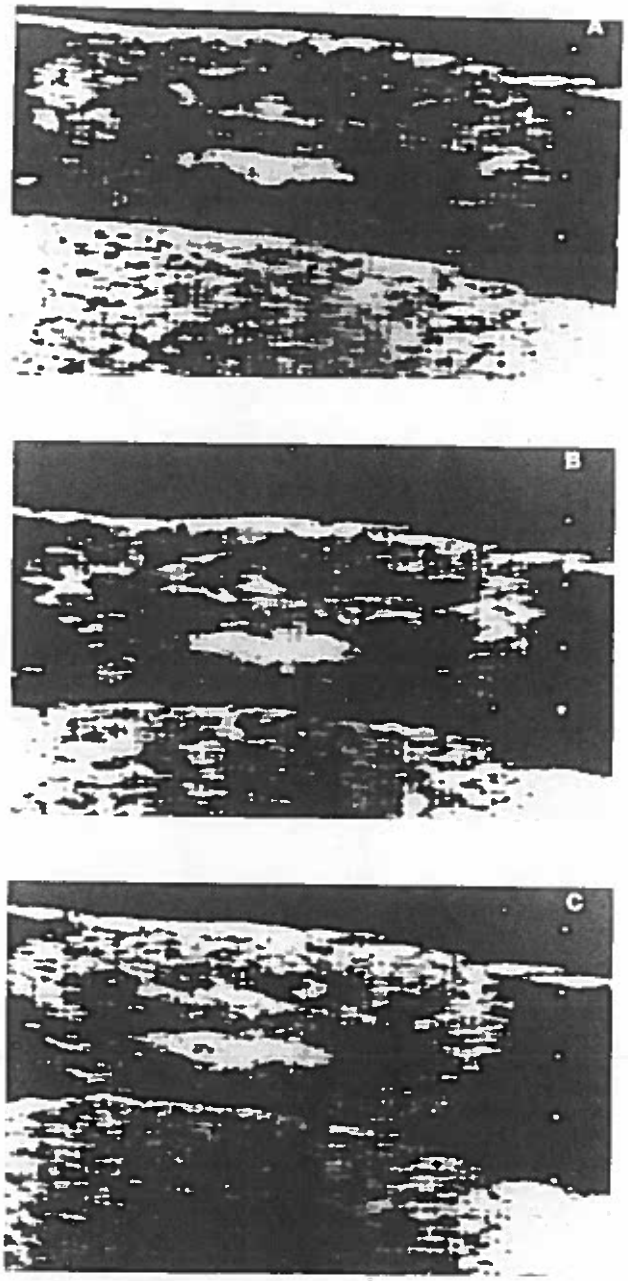

Fig. 7. Echo enhancement in a longitudinal scan of a canine kidney *in vitro* following administration of sodium citrate. (A) Control, (B) Echo enhancement, (C) Maximum effect. Note progressive improvement of visualization of the renal pyramids and increasing shadow in echoes from sponge behind the kidney. (Reprinted with permission from Ophir et al. 1979.)

κ_s = adiabatic compressibility of the scatterer,
κ = adiabatic compressibility of the embedding medium,
ρ_s = density of the scatterer,
ρ = density of the embedding medium.

The first bracketed quantity simply involves the relationship between the wavelength and the radius of the scatterer. It is seen that the radius of the scatterer is extremely important in the determination of the cross section, as is the wavelength. The second bracketed quantity involves the density and compressibility differences between the scatterer and the embedding medium.

If we assume a constant value for the first bracketed quantity in eqn (5), we can investigate the approximate relative scattering efficiency of gas-, solid-, and liquid-based scatterers. For gas-based scatterers, we assume that $\kappa_s \gg \kappa$ and $\rho_s \ll \rho$. Substituting, we get for the second bracketed quantity in eqn (5)

$$\left[\quad\right] \simeq \left[\left|\frac{\kappa_s}{\kappa}\right|^2 + \frac{1}{3}\left|\frac{3(-\rho)}{-\rho}\right|^2\right]. \tag{6}$$

Using typical values from Table 1, we get, $\left[\quad\right] \simeq 10^{14}$. This does not include possible further increase due to bubble resonance, as described later.

For solid scatterers we assume a limiting case that $\kappa_s \ll \kappa$ and that $\rho_s \gg \rho$. Substituting, we get

$$\left[\quad\right] \simeq \left[\left|\frac{-\kappa}{\kappa}\right|^2 + \frac{1}{3}\left|\frac{3\rho_s}{2\rho_s}\right|^2\right] = 1 + \frac{3}{4} = 1.75. \tag{7}$$

Clearly, the scattering cross section in this case is much smaller than for the case of gas.

Lastly, when we look at liquid based scatterers, we assume that $\kappa_s \simeq \kappa$ and that $\rho_s \simeq \rho$. Substituting, we get

$$\left[\quad\right] \simeq 0, \tag{8}$$

i.e., we expect very little or no backscatter enhancement. However, since unlike solid scatterers, liquids could in principle occupy the full diameter of the vessel through which they flow, the assumption that the first bracketed term in eqn (5) is constant can be relaxed to accommodate the larger effective size of a liquid scatterer. Since σ is proportional to a^6 as long as Rayleigh scattering is maintained, the first bracketed term may greatly increase in going from a small scatterer diameter ($\sim$1 micron) to small vessel diameter ($\sim$100 micron). Thus under such circumstances contrast may occur due to the presence of liquid-based agents in blood vessels.

For a cloud of small scatterers in low concentration with individual scattering cross section σ, the effective scattering cross section

$$\sigma_{\text{eff}} = m\sigma, \tag{9}$$

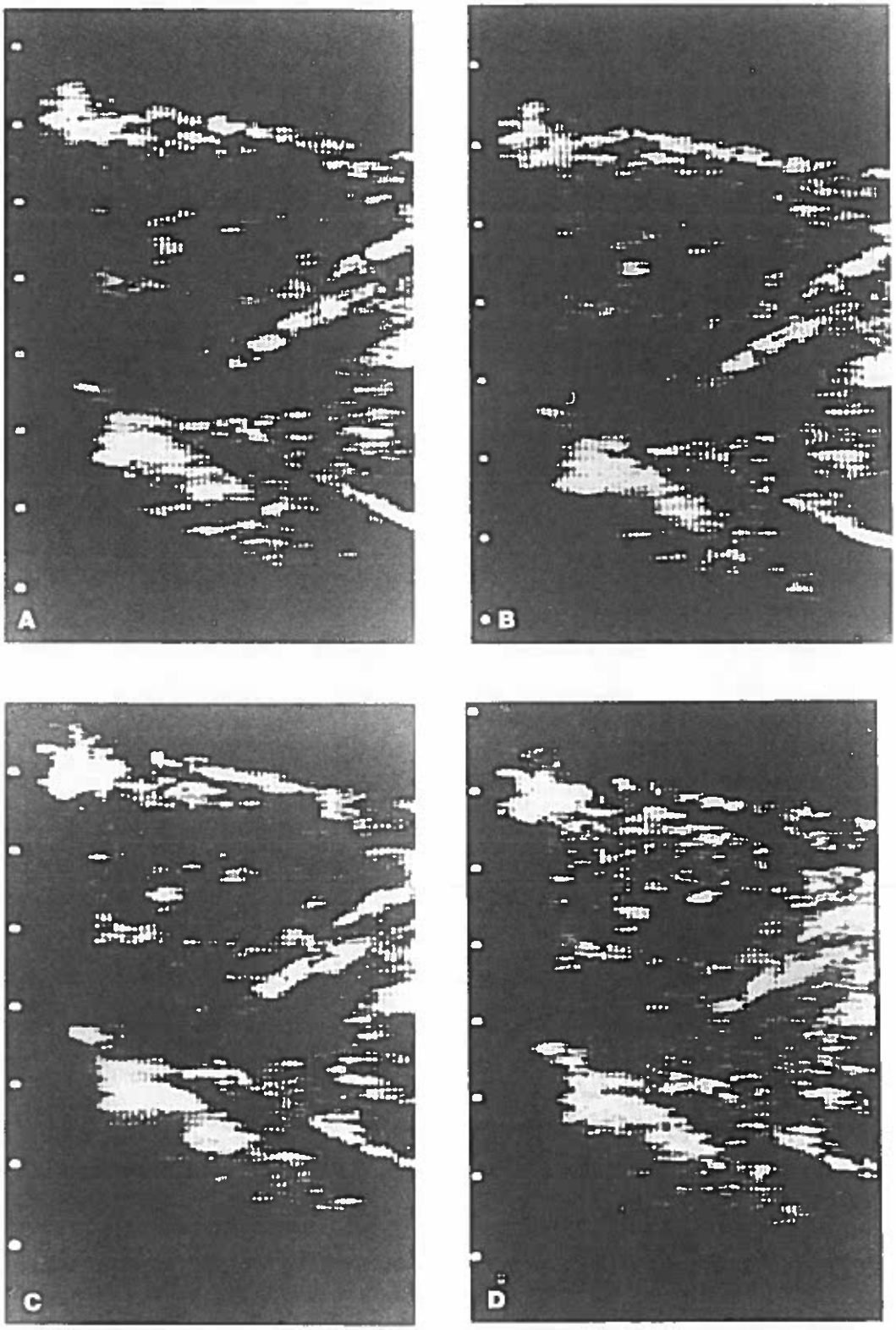

Fig. 8. Longitudinal scan of exposed canine kidney *in vivo*. (A) Control pre-injection of physiological saline. (B) Post-injection of saline. Note no observable effect. (C) Pre-injection of sodium citrate. (D) Post-injection of sodium citrate. Note improved cortical to medullary contrast. (Reprinted with permission from Ophir et al. 1979.)

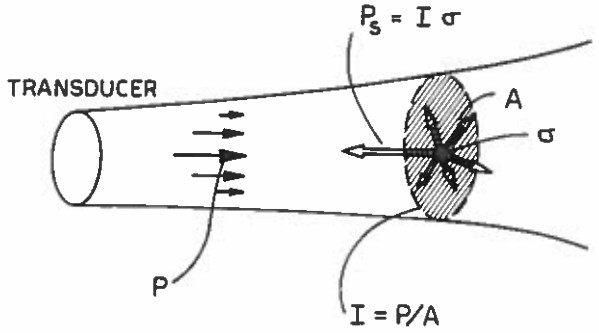

Fig. 9. Scattering from a small particle. P = power emitted; A = cross sectional area of the beam at the range of the scatterer; I_i = intensity of incident beam at the location of the scatterer; σ = scattering cross section; P_s = backscattered power.

where m is the total number of scatterers in the insonified volume (Newhouse et al. 1980). It is therefore possible to increase scattering linearly with increasing concentration of scatterers. Note, however, that this is much less effective than increasing the diameter and/or the frequency due to the strong power law dependence on these parameters.

2. *Bubble resonance phenomena*

Free gas bubbles in a liquid are capable of strong oscillatory motion, and therefore, theoretical treatments of backscatter (and attenuation) require a different approach from the earlier treatment (Section III.1.) of long-wavelength scattering from fluid or solid inhomogeneities.

It is possible to treat small amplitude, radial pulsations of bubbles in an ultrasound field using linear theory in which spring-mass-damping terms can be identified. The bubble then acts like a harmonic oscillator with resonance frequency

$$f_0 = \frac{1}{2\pi a}\sqrt{\frac{3\gamma p_0}{\rho_0}} \qquad (10)$$

Table 1. Compressibility and density of some biological and nonbiological materials. (Shung et al. 1976; Newhouse et al. 1980; Parker et al. 1987).

Material	Compressibility (κ) (cm^2/dyne)	Density (ρ) (g cm^{-3})
Air	2.3×10^{-4}	1.29×10^{-3}
Water	4.6×10^{-11}	1.00
Erythrocyte	3.4×10^{-11}	1.09
Aluminum	1.3×10^{-12}	2.7
IDE	2×10^{-12} (est.)	2.4
Nickel	5×10^{-13}	8.8

where a is the bubble radius (assumed to be small compared to the wavelength), γ is the adiabatic ideal gas constant, and p_0, ρ_0 are ambient fluid pressure and density, respectively (Kinsler et al. 1982).

The above equation gives resonance frequencies below 1 MHz for bubbles larger than 10 μm, while smaller bubbles, on the order of 5 microns or less, have resonances in the medical imaging band of 1–10 MHz.

A bubble in resonance can have a scattering and absorption cross section over a thousand times greater than the physical size, thus producing dramatic effects on the propagating ultrasonic wave. This scattered energy can be so strong that detectability of isolated individual resonant bubbles *in vivo* has been proposed and investigated (Mackay and Rubissow 1978; ter Haar and Daniels 1981).

Resonant bubbles are difficult to use in practice, however. The resonant size for conventional imaging frequencies is in the micron range, but free (unencapsulated) bubbles of this size are unstable, dissolving into surrounding unsaturated water or blood within 100 ms or so (Crum 1985) under the compressive force of surface tension. If bubbles are encapsulated to stabilize them (Feinstein et al. 1984), then the effective mass, stiffness and damping properties change, affecting both the resonant frequency and the strength of response (see, *e.g.*, Miller and Nyborg 1983; Neppiras et al. 1983). If larger, stable bubbles on the order of 10–500 μm are injected into the major vessels, then enhanced backscatter is seen because of the large size and high impedance mismatch presented by the bubbles, and not because of resonant behavior. Though quite useful for cardiac studies (Gramiak and Shah 1968; Gramiak et al. 1969), bubbles larger than 3–5 μm will not pass through the capillary system of the lungs and therefore are not distributed to body organs.

IV. ATTENUATION CONTRAST MECHANISMS

Ultrasound contrast agents are commonly expected to increase tissue backscatter; however, changes in attenuation may also prove to be quite useful. It is germane to point out that extreme differences in attenuation between a lesion and surrounding tissue can be inferred from conventional B-scan images by the "shadowing" or "enhancement" below the lesion (Kremkau and Taylor 1986), and that this effect has been helpful in diagnosis. Furthermore, it is interesting to note that x-ray contrast agents are based on increased beam attenuation. CT images made before and after contrast injections can be examined for

local changes in attenuation, measured in Hounsfield units. Similar techniques may be applied as ultrasound attenuation images become feasible. Currently, the major restriction on acceptable ultrasound attenuation images is the requirement for large regions of interest so that acoustic speckle fluctuations can be averaged out. Typically, regions ranging in area from 1 to 20 cm^2 are required for accurate attenuation estimates (Parker et al. 1987).

Even with these restrictions, it has been possible to show localized attenuation differences between a hemangioma and surrounding liver tissue of a patient, and, in another case, the attenuation difference between liver and adjacent spleen tissue, as shown in Fig. 10, using only 2×2 cm^2 regions of interest and signal processing techniques which are described elsewhere (Parker and Waag 1983; Parker et al. 1984; Parker et al. 1988). The possibility of quantitative attenuation images has been explored, and preliminary results have been encouraging (Walach et al. 1986). Thus, it is feasible that comparison of tissue attenuation before and after the introduction of contrast agents will yield additional diagnostic information.

The mechanisms of increased attenuation which results from the addition of solid particles to tissue include scattering and relative motion. Longitudinal wave scattering by the particles (eqn 5) is responsible for the increased backscatter and results in a small loss, or attenuation of the ultrasound pulse. However, for particles such as dense IDE spheres (Parker et al. 1987), the losses due to scattering are over two orders of magnitude below losses due to relative motion, which describes the viscous losses caused by the difference between the displacements of particle and surrounding medium.

Under a number of assumptions (Parker et al. 1987; Carstensen and Schwan 1959; Fry 1952; Allegra and Hawley 1972) the attenuation caused by relative motion can be shown to be proportional to:

$$\alpha = N\left(\frac{\rho_s - \rho}{\rho}\right)^2 f(a, \omega, \eta, \rho) \qquad (11)$$

where N is the number of particles per unit volume, ρ_s and ρ are the particle and tissue (fluid) densities, and $f(\cdot)$ is a complicated function of particle radius a, frequency ω, fluid viscosity η, and density ρ.

The theory of relative motion provided a good match to measured values of IDE particles in agar, as shown in Fig. 11, however results were different for IDE particles in excised rat liver, as shown in Fig. 12. One additional factor in rat liver is the agglomeration of particles by Kupffer cells, which may produce a larger "effective" particle diameter and other effects (Parker et al. 1987; Lerner et al. 1988). At non-lethal doses used to enhance liver backscatter by IDE particles, the attenuation increase shown in Fig. 10 is greater than 10% over a wide range of frequencies, a sufficient attenuation change for detectability using current *in vivo* attenuation estimators (Parker 1986).

Attenuation changes by injected fluids are more

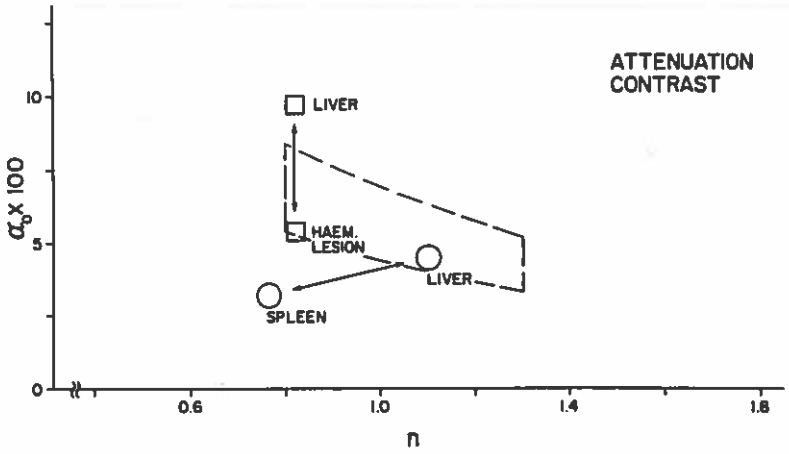

Fig. 10. Values of attenuation within different regions of two abdominal B-scans. In one case, attenuation within a 3 cm diameter haemangioma is lower than that of the surrounding liver. In another case, attenuation within an enlarged spleen was found to be lower than that in the patient's liver. Attenuation values are plotted as a two parameter power law fit, where α_0 is the magnitude and n the frequency dependence of attenuation, and where the dotted line indicated the region of normal liver values according to the methods of Parker et al. (1988). These results indicate that attenuation estimates can reveal underlying difference between neighboring regions of tissue, regardless of whether the region is hyperechoic (as in the haemangioma lesion) or hypoechoic (as in the spleen) compared to normal liver. (Parker, K. J. Unpublished material.)

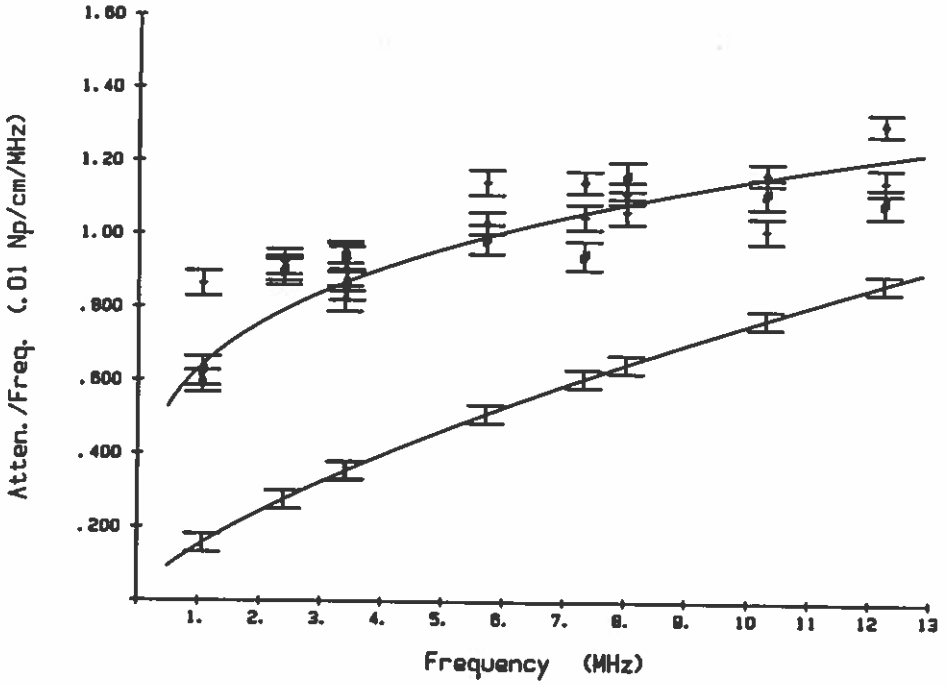

Fig. 11. Attenuation (divided by frequency) versus frequency for plain 2% agar (lower), and agar with 3.2 mg/cc of 1.0 μm IDE particles (mean and 1 *sd* shown for three different samples of 3.2 mg/cc particle suspensions). The solid line for agar represents a curve fit, whereas the solid line for agar-IDE suspensions (top) is a theoretical curve obtained using relative motion to predict the excess attenuation caused by 1.0 μm particles. This theory provides a good description of the magnitude and frequency dependence of attenuation of IDE suspensions in agar. (Reprinted with permission from Parker et al. 1987.)

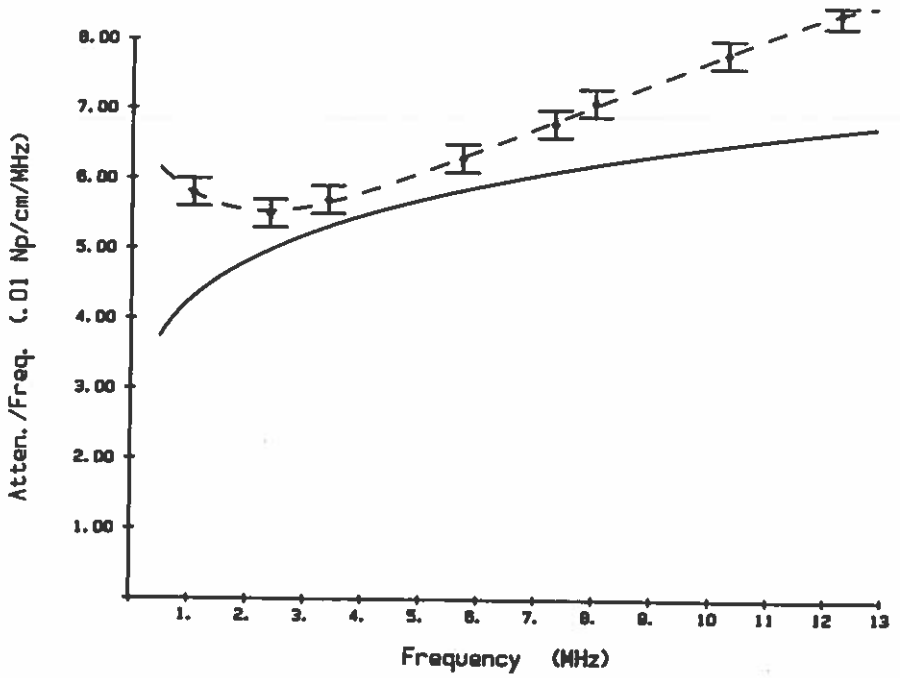

Fig. 12. Attenuation (divided by frequency) versus frequency for normal rat livers with approximately 1.6 mg/cc of 1.0 μm IDE particles, excised 2 hours following intravenous injection of particulate suspension. Solid line (lower) is a power law curve fit to mean values of 25 normal livers (*sd* ± 7% not shown). Data points (upper) are mean and single *sd* for a group of 4 livers with IDE particles. The excess attenuation resulting from particle uptake in liver is different from that found in agar, possibly indicating additional interactions such as the aggregation of particles by Kupffer cells. (Reprinted with permission from Parker et al. 1987.)

difficult to analyze because of the complex distribution within the vasculature. However, a highly attenuating fluid perfused into the capillary bed of an organ could increase bulk attenuation, through simple mixture rules. The resulting attenuation coefficient would be, to first order, the sum of the individual attenuation coefficients, times their volume fractions x, that is,

$$\alpha = x_f \alpha_f + x_t \alpha_t, \tag{12}$$

where

$$x_f + x_t = 1, \tag{13}$$

and where the subscripts f and t refer to contrast fluid and tissue, respectively.

Even at low concentrations, absorption due to resonant bubbles in tissue may be sufficiently large (Nyborg 1985) as to possibly degrade imaging by limiting penetration depth. However, as mentioned previously, free resonant bubbles which are small enough to pass through the capillary bed are unstable, and coated microbubbles will require further analysis for attenuation properties.

V. SPEED OF SOUND CONTRAST MECHANISMS

In addition to backscatter and attenuation, the use of the speed of sound parameter and its dependence on the presence of a contrast agent is an interesting possibility. Apparatus for the measurement of speed of sound *in vivo* exist experimentally (Robinson et al. 1982; Bamber and Abbott 1985; Iinuma et al. 1985; Katakura et al. 1985; Hayashi et al. 1985; Ohtsuki et al. 1985; Ophir 1986). Potential contrast agents which have low (Mattrey et al. 1983) or high (McWhirt 1979) speed of sound relative to tissue have been described.

A suspension of solid particles in a liquid, or of liquid droplets in a liquid, produces an increase of damping and a change of velocity of sound in the mixture. If the particles suspended in the liquid are sufficiently small compared to the ultrasound wavelength, the composite medium may for convenience be regarded as homogeneous and the fine structure of sound transmission ignored (Wood 1964).

To determine the velocity of sound in the composite we assume that the velocity is the same as the homogeneous fluid of the same mean density and mean compressibility as in the composite (Wood 1964). Let ρ_1, κ_1, and ρ_2, κ_2 represent the density and the compressibility of the constituents 1 and 2, respectively. Then let x = the proportion of the first constituent by volume and $(1 - x)$ = the proportion of the second constituent by volume. The mean density ρ is therefore

$$\rho = x\rho_1 + (1 - x)\rho_2. \tag{14}$$

The compressibilities add is a manner analogous to resistances in parallel, that is,

$$\frac{1}{\kappa} = \frac{x}{\kappa_1} + \frac{(1 - x)}{\kappa_2}, \tag{15}$$

from which the mean compressibility

$$\kappa = \frac{\kappa_1 \kappa_2}{x\kappa_2 + (1 - x)\kappa_1}. \tag{16}$$

Therefore the mean velocity of sound

$$c = \left(\frac{\kappa}{\rho}\right)^{1/2} = \left\{\frac{\kappa_1 \kappa_2}{[x\kappa_2 + (1 - x)\kappa_1][x\rho_1 + (1 - x)\rho_2]}\right\}^{1/2}. \tag{17}$$

If we assume that the density and compressibility of the tissue are approximately known, and that the contrast materials are well characterized, measurable changes in the speed of sound in the tissue allow calculation of the amount of contrast material which is present in the tissue. This quantitative attribute of speed of sound contrast would make it suitable for temporal tissue perfusion studies.

As an example, some of the fluorocarbon materials can be injected in large amounts (Mattrey et al. 1983) and have speeds of sound on the order of 600 m s^{-1}. If 2% of the target organ volume is displaced by such a material, approximately a 1% reduction of the speed of sound in the tissue will result. Such a change should be measurable using some current experimental methods (Ophir 1986).

VI. CONTRAST VS. TOXICITY

Since contrast enhancement depends on the administration of a quantity of contrast material into a biological system, the attainable contrast is ultimately limited by the short- and long-term toxic effects of such substances. Thus a quality factor for contrast agents may be defined as

$$Q = \left|\frac{\text{contrast enhancement/dose}}{\text{toxicity/dose}}\right|. \tag{18}$$

Contrast enhancement may be defined as the maxi-

Table 2. Advantages and disadvantages of free gas bubbles.

Free gas bubbles
Advantages
1. Extremely efficient backscatter enhanced even at small size and concentration
2. Potential low toxicity
3. Could be used for right heart, bile ducts
Disadvantages
1. No transpulmonary transport–not suitable for soft tissue contrast
2. Short half-life

mum percent change in the contrast effect due to the introduction of the contrast material. Toxicity may be defined in many ways; one way is the inverse of the LD_{50}, which is the dose which is lethal to 50% of the experimental animals. It appears from the above equation that the dose can be canceled out. However, both contrast enhancement and toxicity may in general be nonlinearly related to dose. Thus Q itself is a function of dose, and a more precise way to define Q at any given dose is

$$Q(\text{dose}) = \left|\frac{\text{contrast enhancement}}{\text{toxicity}}\right|_{\text{dose}}. \quad (19)$$

In order to increase Q, one can strive to increase the numerator and/or decrease the denominator of this quotient. Increasing the numerator has been discussed previously. Decreasing the denominator can be attempted in a variety of ways (Gobuty 1987). These include

1. Change in the rate of administration of the agent,
2. Simultaneous administration of a buffering compound which reduces the toxicity of the contrast agent alone,
3. Change in the route of administration, and
4. Increase in the rate of elimination of the agent via other drugs.

Table 3. Advantages and disadvantages of encapsulated gas bubbles.

Encapsulated gas bubbles
Advantages
1. Efficient scatterers
2. Potential low toxicity
3. Small sizes (<2 μm) could be used for soft tissue contrast
Disadvantages
1. Difficult to manufacture in small sizes due to leakage
2. Larger sizes are of limited use

Table 4. Advantages and disadvantages of colloidal suspensions.

Colloidal suspensions
Advantages
1. Could be used for soft tissue backscatter contrast (liver, spleen?)
2. Relatively efficient scatterers
3. Long half life
4. Possibility of attenuation contrast
5. Possibility of selective biodistribution
6. Possibility of enhanced scatter from clumping in Kupffer cells
Disadvantages
1. Toxicity may be high
2. Long half life

In addition to these factors, other variables may be controlled which will reduce the dose required to elicit contrast. Sensitivity of the instrumentation to contrast effects can be increased by using quantitative measures for estimating the enhancement of backscatter, and by employing image subtraction techniques (as used in angiography) to greatly emphasize small changes in such backscatter (Gobuty et al. 1988).

VII. CONCLUSION

We have reviewed various classes of ultrasound contrast agents. The basic acoustic mechanisms of scattering, attenuation, and speed of sound have been presented so that relative merits of gas bubbles, solid particles, fluids, and other agents can be compared.

It should be stressed that the use of ultrasound contrast agents today is essentially experimental. This is due to the many practical difficulties with identifying and manufacturing suitable "high Q" contrast agents, the scarcity of equipment for quantifying their effect, and the significant effort required to characterize their biodistribution and toxicity.

Tables 2 through 5 list the advantages and disadvantages of the main classes of contrast agents. Given the wide range of clinical objectives such as opacifi-

Table 5. Advantages and disadvantages of emulsions and solutions.

Emulsions/Solutions
Advantages
1. Could be used for soft tissue contrast (kidney?)
2. Possibility of dynamic studies
3. Possibility of speed of sound contrast
Disadvantages
1. Toxicity may be high
2. Relatively inefficient scatterers (but presence in large vessels could compensate)

cation of luminal boundaries, blood flow markers and soft tissue enhancement and differentiation, it is unlikely that any single class of materials will function as a universal ultrasound contrast agent. The clinical need for ultrasound contrast agents is high, but much interdisciplinary research, covering acoustic material properties, imaging, biochemistry, histology, toxicology, and related specialties will be required before ultrasound contrast agents are commercially available and in routine clinical use.

Acknowledgment—This work was supported in part by National Institutes of Health Contract #N01-CB 84236 and Grant #R01-CA 44732.

REFERENCES

Allegra, J. A.; Hawley, S. A. Attenuation of sound in suspensions and emulsions. J. Acoust. Soc. Am. 51:1545–1564; 1972.

Armstrong, W. F.; Mueller, T. M.; Kinney, E. L.; Tickner, E. G.; Dillon, J. C.; Feigenbaum, H. Assessment of myocardial perfusion abnormalities with contrast-enhanced two-dimensional echocardiography. Circulation 66(1):166–173; 1982.

Armstrong, W. F.; West, S. R.; Mueller, T. M.; Dillon, J. C.; Feigenbaum, H. Assessment of location and size of myocardial infarction with contrast-enhanced echocardiography. J. Am. Coll. Cardiol. 2(1):63–69; 1983.

Armstrong, W. F.; West, S. R.; Dillon, J. C.; Feigenbaum, H. Assessment of location and size of myocardial infarction with contrast-enhanced echocardiography. II. Application of digital imaging techniques. J. Am. Coll. Cardiol. 4(1):141–148; 1984.

Bamber, J. C.; Abbott, C. The feasibility of measuring average speed of sound in tissues using a real-time scanner. In: Gill, R. A.; Dadd, M. J., eds. Proc. Fourth World Fed. Ultrasound Med. Biol. New York: Pergamon; 1985:517 (abstract).

Brown, A. K.; Anderson, V. The value of contrast cross-sectional echocardiography in the diagnosis of tricuspid regurgitation. Eur. Heart J. 5(1):62–66; 1984.

Carroll, B. A.; Turner, R. J.; Tickner, E. G.; Boyle, D. B.; Young, S. W. Gelatin encapsulated nitrogen microbubbles as ultrasonic contrast agents. Invest. Radiol. 15(3):260–266; 1980.

Carstensen, E. L.; Schwan, H. P. Absorption of sound arising from the presence of intact cells in blood. J. Acoust. Soc. Am. 31:185–189; 1959.

Chiang, C. W.; Lin, F. C.; Fu, M.; Fang, B. R.; Hsu, T. S.; Lee, Y. S. Importance of adequate gas-mixing in contrast echocardiography. Chest 89(5):723–726; 1986.

Crum, L. Acoustic cavitation. Notes for short course at Rochester Center for Biomedical Ultrasound; 1985.

Feinstein, S. B.; Ten-Cate, F. J.; Zwehl, W.; Ong, K.; Maurer, G.; Tei, C.; Shah, P. M.; Meerbaum, S.; Corday, E. Two-dimensional contrast echocardiography. I. *In vitro* development and quantitative analysis of echo contrast agents. J. Am. Coll. Cardiol. 3(1):14–20; 1984.

Fink, I. J.; Miller, D. J.; Shawker, T. H. Lipid emulsions as contrast agents for hepatic sonography: an experimental study in rabbits. Ultrasonic Imaging 7:191–197; 1985.

Fry, W. F. Mechanism of acoustic absorption in tissue. J. Acoust. Soc. Am. 24:412–415; 1952.

Gillam, L. D.; Kaul, S.; Fallon, J. T.; Levine, R. A.; Hedley-Whyte, E. T.; Guerrero, J. L.; Weyman, A. E. J. Am. Coll. Cardiol. 6(3):687–694; 1985.

Gobuty, A. H. Perspectives in ultrasound contrast agents. In: Parvez, Z., ed. Contrast media: biologic effects and clinical applications. Boca Raton, FL: CRC Press; 1987: Chap. 34.

Gobuty, A. H.; Ophir, J.; Irvine, R.; Wu, I. C.; Yazdi, Y.; Johnson, W.; Kontonassios, T. Enhanced backscatter imaging in a living rabbit using intravenous buffered contrast agents. Ultrasonic Imaging 10(1):68–69; 1988 (abstract).

Goldberg, B. B. Ultrasonic cholangiography. Radiology 118:401–404; 1976.

Gramiak, R.; Shah, P. M. Echocardiography of the aortic root. Investigative Radiology 3:356–366; 1968.

Gramiak, R.; Shah, P. M.; Kramer, P. H. Ultrasonic cardiography: contrast studies. Radiology 92:939; 1969.

Haar, G. ter; Daniels, S. Physics in Med. and Biol. 26:1145; 1981.

Hayashi, N.; Tamaki, N.; Yamamoto, K.; Senda, M.; Yonekura, Y. et al. *In vivo* measurement of sound speed in normal and abnormal livers using a high resolution ultrasonic scanner. In: Gill, R. W.; Dadd, M. J., eds. Proc. Fourth World Fed. Ultrasound Med. Biol. New York: Pergamon; 1985:520 (abstract).

Iinuma, K.; Sumino, Y.; Hirama, M.; Okazaki, K.; Sato, T. et al. A proposal of crossed beam method using a linear array probe for *in vivo* measurement of sound velocity of tissue. In: Gill, R. W.; Dadd, M. J., eds. Proc. Fourth World Fed. Ultrasound Med. Biol. New York: Pergamon; 1985:515 (abstract).

Katakura, K. *In vivo* sound speed measurement in the reflection mode. In: Gill, R. W.; Dadd, M. J., eds. Proc. Fourth World Fed. Ultrasound Med. Biol. New York: Pergamon; 1985:516 (abstract).

Kinsler, L. E.; Frey, A. R.; Coppens, A. B.; Sanders, J. V. Fundamentals of acoustics. 3rd ed. New York: Wiley and Sons; 1982.

Kondo, S.; Tei, C.; Meerbaum, S.; Corday, E.; Shah, P. M. Hyperemic response of intracoronary contrast agents during two-dimensional echographic delineation of regional myocardium. J. Am. Coll. Cardiol. 4:149–156; 1984.

Kremkau, F. W.; Carstensen, E. L. Ultrasonic detection of cavitation at catheter tips. Am. J. Roentgenol. 3:159; 1968.

Kremkau, F. W.; Taylor, K. J. W. Artifacts in ultrasound imaging. J. Ultrasound in Medicine 5:227–237; 1986.

Lerner, R. M.; Gramiak, R.; Violante, M. R.; Parker, K. J. Ultrasound contrast agents. In: Skucas, J., ed. Radiographic contrast agents. 2nd ed. Aspen Publishers; 1988.

Levine, R. A.; Teichholz, L. E.; Goldman, M. E.; Steinmetz, M. Y.; Baker, M.; Meltzer, R. S. Microbubbles have intracardiac velocities similar to those of red blood cells. J. Am. Coll. Cardiol. 3(1):28–33; 1984.

Mackay, R. S.; Rubissow, G. Decompression studies using ultrasonic imagery of bubbles. IEEE Trans. BME-25:537–544; 1978.

Mattrey, R. F.; Scheible, F. W.; Gosink, B. B.; Leopold, G. R.; Long, D. M.; Higgins, C. B. Perfluorooctyl bromide: a liver-spleen specific and tumor-imaging ultrasound contrast material. Radiology 145:759–762; 1982.

Mattrey, R. F.; Leopold, G. R.; von Sonnenberg, E.; Gosink, B. B.; Scheible, F. W.; Long, D. Perfluorochemicals as liver and spleen-seeking ultrasound contrast agents. J. Ultrasound Med. 2:173–176; 1983.

Mattrey, R. F.; Strich, G.; Shelton, R. E.; Gosink, B. B.; Leopold, G. R.; Lee, T.; Forsythe, J. Perfluorochemicals in US contrast agents for tumor imaging and hepatosplenography: preliminary clinical results. Radiology 163:339–343; 1987.

Maurer, B.; Ong, K.; Haendchen, R.; Torres, M.; Tei, C.; Wood, F.; Meerbaum, S.; Shah, P.; Corday, E. Myocardial contrast two-dimensional echocardiography: comparison of contrast disappearance rates in normal and underperfused myocardium. Circulation 69(2):418–429; 1984.

McWhirt, R. E. Speed of sound measurements in potential contrast agents for use in diagnostic ultrasound. University of Kansas; 1979. Masters thesis.

Meltzer, R. S.; Serruys, P. W.; McGhie, J.; Verbaan, N.; Roelandt, J. Pulmonary wedge injections yielding left-sided echocardiographic contrast. Br. Heart J. 44(4):390–394; 1980a.

Meltzer, R. S.; Tickner, E. G.; Popp, R. L. Why do the lungs clear ultrasonic contrast? Ultrasound Med. Biol. 6(3):263–269; 1980b.

Meltzer, R. S.; Serruys, P. W.; Hugenholtz, P. G.; Roelandt, J. Intravenous carbon dioxide as an echocardiographic contrast agent. J. Clin. Ultras. 9(3):127–131; 1981.

Meltzer, R. S.; Klig, V.; Teichholz, L. E. Generating precision

microbubbles for use as an echocardiographic contrast agent. J. Am. Coll. Cardiol. 5(4):978–982; 1985.
Meyer-Schwickerath, M.; Fritzsch, T. Sonographic imaging of the kidney cavity system using ultrasonic contrast medium. Ultraschall Med. 7:34–36; 1986.
Miller, D. L.; Nyborg, W. L. Theoretical investigation of response of gas-filled micropores and cavitation nuclei to ultrasound. J. Acoust. Soc. Am. 73:1537–1544; 1983.
Morse, P. M.; Ingard, K. U. Theoretical acoustics. New York: McGraw Hill; 1968:427.
Munoz, S.; Berti, C.; Pulido, C.; Blanco, P. Two dimensional contrast echocardiography with carbon dioxide in the detection of congenital cardiac shunts. Am. J. Cardiol. 53(1):206–210; 1984.
Neppiras, E. A.; Nyborg, W. L.; Miller, P. L. Nonlinear behavior and stability of trapped micron-sized cylindrical gas bubbles in an ultrasound field. Ultrasonics 21:109–115; 1983.
Newhouse, V. L.; Hoover, M. L.; Ash, S. R. The detection of blood impurities using ultrasound Doppler. Ultrasonic Imaging 2:370–380; 1980.
Nyborg, W. L. Bubble dynamics and cavitations. Notes for short course at Rochester Center Biomedical Ultrasound; 1985.
Ohtsuki, S.; Soetanto, K.; Okujima, M. A technique with reference points image for *in vivo* measurement of sound velocity. In: Gill, R. W.; Dadd, M. J., eds. Proc. Fourth World Fed. Ultrasound Med. Biol. New York: Pergamon; 1985:521 (abstract).
Ophir, J.; McWhirt, R. E.; Maklad, N. F. Aqueous solutions as potential ultrasonic contrast agents. Ultrasonic Imaging 1:265–279; 1979.
Ophir, J. Estimation of speed of ultrasound propagation in biological tissues: a beam tracking method. IEEE Trans. Ultrason. Ferroelect., Freq. Contr. UFFC-33:359–368; 1986.
Ophir, J.; Gobuty, A.; McWhirt, R. E.; Maklad, N. F. Ultrasonic backscatter from contrast producing collagen microspheres. Ultrasonic Imaging 2:67–77; 1980.
Ophir, J.; Gobuty, A.; Maklad, M. F.; Tyler, T.; Jaeger, P.; McWhirt, R. E. Quantitative assessment of *in vivo* backscatter enhancement from gelatin microspheres. Ultrasonic Imaging 7:293–299; 1985.
Parker, K. J.; Waag, R. C. Measurement of ultrasonic attenuation within regions selected from B-scan images. IEEE Trans. Biomed. Engr. BME 30(8):431–437; 1983.
Parker, K. J.; Lerner, R. M.; Waag, R. C. Attenuation of ultrasound magnitude and frequency dependence for tissue characterization. Radiology 153(3):785–788; 1984.
Parker, K. J. Attenuation measurement uncertainties caused by speckle statistics. J. Acoust. Soc. Am. 80(33):727–734; 1986.
Parker, K. J.; Tuthill, T. A.; Lerner, R. M.; Violante, M. R. A particulate contrast agent with potential for ultrasound imaging of liver. Ultrasound Med. Biol. 13(9):555–566; 1987.
Parker, K. J.; Aaztely, M. S.; Lerner, R. M.; Schenk, E. A.; Waag, R. C. *In vivo* measurements of ultrasound attenuation in normal or diseased livers. Ultras. Med. Biol. 14(2):127–136; 1988.
Rizayev, M. N.; Azatyan, T. S. Contrast echocardiography by protein-carbonate foam. Heart J. 10(6):1308–1310; 1985.
Robinson, D. E.; Chen, F.; Wilson, L. S. Measurement of velocity of propagation from ultrasonic pulse echo data. Ultrasound Med. Biol. 8:415–420; 1982.
Shung, K. K.; Sigelman, R. A.; Reid, J. M. Scattering of ultrasound by blood. IEEE Trans. Biomed. Engr. BME 23(6):460–467; 1976.
Tei, C.; Sakamaki, T.; Shah, P. M.; Meerbaum, S.; Shimoura, K.; Kondo, S.; Corday, E. Myocardial contrast echocardiography: a reproducible technique of myocardial opacification for identifying regional perfusion deficits. Circulation 67(3):585–593; 1983.
Tei, C.; Kondo, S.; Meerbaum, S.; Ong, K.; Maurer, G.; Wood, F.; Sakamaki, T.; Shimoura, K.; Corday, E.; Shah, P. M. Correlation of myocardial echo contrast disappearance rate ("washout") and severity of experimental coronary stenosis. J. Am. Coll. Cardiol. 3(1):39–46; 1984.
Ten-Cate, F. J.; Feinstein, S.; Zwehl, W.; Meerbaum, S.; Fishbein, M.; Shah, P. M.; Corday, E. Two-dimensional contrast echocardiography. II. Transpulmonary studies. J. Am. Coll. Cardiol. 3(1):21–27; 1984.
ter Haar, G.; Daniels, S. Evidence for ultrasonically induced cavitation in vivo. Phys. Med. Biol. 26:1145–1149; 1981.
Tyler, T. D.; Ophir, J.; Maklad, N. F. *In vivo* enhancement of ultrasonic image luminance by aqueous solutions with high speed of sound. Ultrasonic Imaging 3:323–329; 1981.
Violante, M. R.; Fischer, H. W.; Mahoney, J. Particulate contrast media. Invest. Radiol. 15:329; 1980.
Walach, E.; Lin, C. N.; Waag, R. C.; Parker, K. J. Quantitative tissue characterization. IEEE Trans. Biomed. Engr. BME 33(7):637–643; 1986.
Wise, N. K.; Myers, S.; Fraker, T. D.; Stewart, J. A.; Kisslo, J. A. Contrast M-mode ultrasonography in the inferior vena cava. Circulation 63(5):1100–1103; 1981.
Wood, A. B. Textbook of Sound. London: G. Bell and Sons, Ltd.; 1964.
Ziskin, M. C.; Bonakdapour, A.; Weinstein, D. P.; Lynch, P. R. Contrast agents for diagnostic ultrasound. Invest. Radiol. 7:500–505; 1972.